INTERNATIONAL JOURNAL OF AUTOMOTIVE SCIENCE AND TECHNOLOGY

2022, VOL. 6, NO: 2, 202-206 www.ijastech.org e-ISSN: 2587-0963

Optimization of a B-Pillar with Tailored Properties Under Impact Loading

İsmail Öztürk[1]

0000-0003-2641-5880

[1] *Automotive Engineering Department, Faculty of Technology, Pamukkale University, Denizli, 20020, Türkiye*

Abstract

Within the study's scope, the impact performance of a boron steel B-pillar with three different hardness values and six different B-pillar designs with tailored properties was compared in crashworthiness. Impact simulation results were compared in terms of specific energy absorption and peak crushing force values of the B-pillar. "Upper part T500 and lower part O25 heat treated B-pillar" gave the highest specific energy absorption. "Upper part O25 and lower part T25 heat treated B-pillar" resulted in the lowest peak crushing force and gave the second highest specific energy absorption. This pillar was used in optimization studies to maximize specific energy absorption and minimize peak crushing force. The single-objective optimization problem was solved with Adaptive Response Surface Method and Sequential Quadratic Programming methods. Specific energy absorption value increased by 47.7% from 1.32 to 1.95 kJ/kg compared reference design for both techniques. Multi-objective Genetic Algorithm and Global Response Surface Method were utilized to solve the multi-objective optimization problem, and similar Pareto front curves were obtained. For both methods, the optimal B-pillar with max specific energy absorption increased the specific energy absorption by 51.5% from 1.32 to 2.00 kJ/kg compared to the reference design. However, peak crushing force increased 14.9% from 63.7 to 73.2 kN. Optimal B-pillar could be used in the automotive industry.

Keywords: B-pillar; Boron steel; Crashworthiness; Optimization; Spesific energy absorption (SEA); Peak crushing force (PCF); Tailored property

Research Article

https://doi.org/10.30939/ijastech..1109644

Received 27.04.2022
Revised 26.05.2022
Accepted 22.06.2022

* Corresponding author

İsmail Öztürk

ismailozturk@pau.edu.tr

Address: Automotive Engineering Department, Faculty of Technology, Pamukkale University, Denizli, Türkiye

Tel: +903122028653

1. Introduction

In the design of vehicle structural components, studies are being done on light part designs with high impact resistance and meet legal requirements. Side impact accidents are serious accidents that can cause fatalities due to the low survivability space between passenger and vehicle components [1]. 35% of the total deaths in vehicle accidents are due to side crashes [2]. B-pillars are essential in protecting occupants from such accidents (Figure 1).

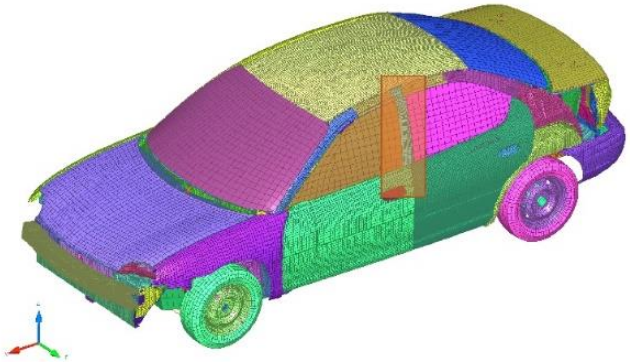

Fig. 1. Location of B-pillar in a vehicle

Although there are many studies on the collision performance of B-pillars in the literature [3-8], studies on the impact performance of hot-formed B-pillars are limited. The collision performance of fully martensitic B-pillar and B-pillar with tailored properties was compared numerically and experimentally. For the tailored B-pillar, the displacement of the impactor was 9% higher and the peak impact force 24% lower than for the fully martensitic [9,10]. Since ductile and strength material properties can be achieved on the same piece with the B-pillar with tailored properties, it is expected to have better collision performance than the fully martensitic material.

This study carried out side impact analyses with a boron steel B-pillar. Analyzes were made for three different homogeneous hardness values and six B-pillar designs with tailored properties. Analysis results were compared regarding specific energy absorption (SEA) and peak crushing force (PCF) values of the B-pillar. "Upper part T500 and lower part O25 heat treated B-pillar" gave the highest SEA. "Upper part O25 and lower part T25 heat treated B-pillar" resulted in the lowest PCF and gave the second highest SEA. This pillar was used in optimization studies to maximize SEA and minimize PCF. This B-pillar can be used on vehicles to improve

crash performance.

2. Side impact analysis

B1500HS boron steel was chosen as the B-pillar material. In the literature, heat treatment was applied to steel sheets at different die temperatures, and different hardness values were obtained. T500 and T25 indicate the die temperature of 500 °C and 25 °C, respectively. The cooling state in an open furnace is called O25 [11]. B-pillar's impact performance was evaluated with three different hardness values and six different pillar designs with tailored properties. The designed B-pillars are shown in Figure 2. The height of the lower part of the B-pillar is 443 mm for tailored designs.

Crash analyses were performed utilizing the B-pillar finite element model of the vehicle crash model in the George Washington University finite element model archive, available to researchers. HyperCrash software was used as a pre-processor in the simulations [12]. The B-pillar thickness has been taken as 1.2 mm, and the 5 mm average element size was preferred. Type 7 and Type 11 contact types were used, and the friction coefficient was chosen as 0.2. Johnson-Cook material model has been used, and Johnson-Cook constants of O25, T500, and T25 heat treated B1500HS boron steel are given in Table 1.

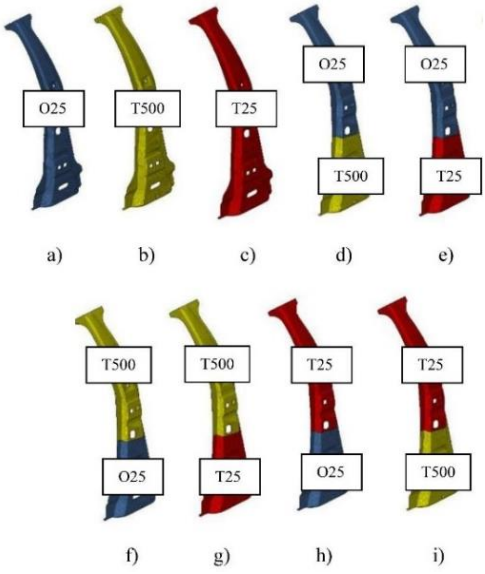

Fig. 2. B-pillar designs:
a) O25 b) T500 c) T25 d) Upper part O25 and lower part T500 e) Upper part O25 and lower part T25 f) Upper part T500 and lower part O25 g) Upper part T500 and lower part T25 h) Upper part T25 and lower part O25 i) Upper part T25 and lower part T500 heat-treated B-pillar

A rigid plate with a square section of 540x540 mm and a mass of 100 kg was impacted on the fixed B-pillar finite element model at a velocity of 10 m/s at a 90° angle. Radioss solver was used for the analysis, and 40 ms was taken as the solution interval to obtain the SEA and PCF values. The side impact model is given in Figure 3. The B-pillar is fixed to the vehicle where it attaches (at the nodes marked red). The displacement contour plot of the O25 heat treated B-pillar at 40 ms is shown in Figure 4. The highest displacement occurred in the middle part, where the rigid plate applied the impact.

Table 1. Johnson-Cook material model constants for O25, T500, and T25 heat treated B1500HS boron steel [11]

Heat treatment type	O25	T500	T25
Density (ton/mm^{-3})	7.85x10^{-9}	7.85x10^{-9}	7.85x10^{-9}
Young's modulus (MPa)	210000	210000	210000
Poisson's ratio	0.33	0.33	0.33
Yield stress (MPa) [a]	305	545	890
Strain hardening coefficient (MPa) [b]	610	695	1150
Strain hardening exponent [n]	0.42	0.4	0.22

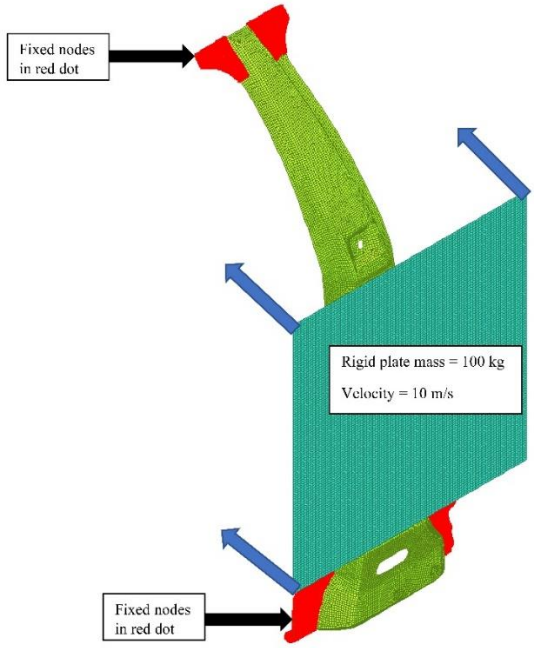

Fig. 3. Side impact finite element model

SEA is the energy absorption of the B-pillar dividing by pillar mass during plastic deformation:

$$SEA = \frac{\int_0^{x_{max}} f(x)dx}{m} \quad (1)$$

In Eq. (1), f(x) is the instantaneous crash force between the rigid plate and the B-pillar, x_{max} is the maximum displacement of the rigid plate, and m is the mass of the B-pillar [13].

PCF is the highest rigid plate force that occurs during the deformation of the B-pillar [14]. A lower PCF value means a lower risk of injury in accidents. The SEA and PCF values obtained from the impact analysis of the pillars are given in Table 2.

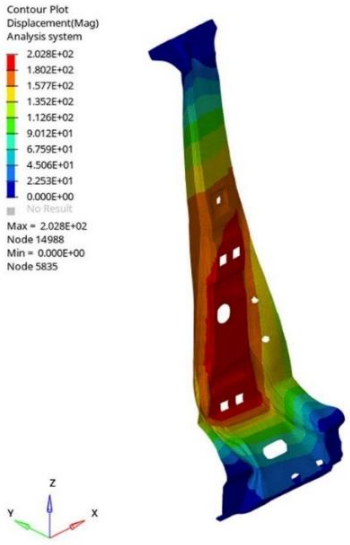

Fig. 4. Displacement results of the model

Table 2. SEA and PCF values of the b-pillars, maximum values shown in bold and italics

Design number	B-pillar type	SEA (kJ/kg)	PCF (kN)
1	O25 heat-treated b-pillar	1.32	76.36
2	T500 heat-treated b-pillar	1.31	79.16
3	T25 heat-treated b-pillar	1.28	78.34
4	Upper part O25 and lower part T500 heat-treated b-pillar	1.32	71.10
5	Upper part O25 and lower part T25 heat-treated b-pillar	1.32	63.70
6	Upper part T500 and lower part O25 heat-treated b-pillar	1.33	83.40
7	Upper part T500 and lower part T25 heat-treated b-pillar	1.31	72.28
8	Upper part T25 and lower part O25 heat-treated b-pillar	1.31	86.26
9	Upper part T25 and lower part T500 heat-treated b-pillar	1.29	91.55

When the table is examined, the highest SEA value was obtained with 1.33 kJ/kg with the sixth design, whereas the lowest PCF value was obtained with 63.7 kN with the fifth design. The SEA value in the fifth design was 1.32 kJ/kg, almost reaching the sixth design. For this reason, the fifth design, "Upper part O25 and lower part T25 heat-treated B-pillar," was used in optimization studies.

3. Optimization studies of B-pillar with tailored properties

In the design of vehicle structural components, the SEA value is expected to be high, while the PCF value is low for passenger safety. Single-objective optimization problem:

$$\begin{aligned} &\text{Objective: Max } SEA(t_u, t_l) \\ &\text{Constraint: } PCF(t_u, t_l) \leq 70 \text{ kN} \\ &\text{Design parameters: } 0.7 \text{ mm} \leq t_u, t_l \leq 1.7 \text{ mm} \end{aligned} \quad (2)$$

with t_u (mm) and t_l (mm): Thicknesses of the O25 and T25 heat treated parts of the B-pillar, respectively. The constraint value for the PCF was selected as 70 kN with optimization based on the simulation results. The multi-objective optimization problem:

$$\begin{aligned} &\text{Objective: Max } SEA(t_u, t_l) \quad \text{Min } PCF(t_u, t_l) \\ &\text{Design parameter } 0.7 \text{ mm} \leq t_u, t_l \leq 1.7 \text{ mm} \end{aligned} \quad (3)$$

Eq. (2) and (3) were solved with different optimization techniques. Design functions are established with the design of experiment (DOE) and response surface methods. The full factorial DOE method was used, nine analyzes were performed, and the results are given in Table 3.

Table 3. DOE simulation results for the B-pillar with tailored properties, results for reference thickness are shown in bold and italics

Experiment no	t_u (mm)	t_l (mm)	SEA (kJ/kg)	PCF (kN)
1	0.7	0.7	2.00	73.20
2	0.7	1.2	1.55	58.64
3	0.7	1.7	1.25	83.65
4	1.2	0.7	1.61	85.87
5	1.2	1.2	***1.32***	***63.70***
6	1.2	1.7	1.10	81.68
7	1.7	0.7	1.35	96.58
8	1.7	1.2	1.14	71.00
9	1.7	1.7	0.99	75.76

Radial Basis Function (RBF), Least Squares Regression (LSR), and Moving Least Squares (MLSM) response surface methods were used [15]. RBF method utilizes linear combinations of basis functions, such as linear and cubic. These basis functions have been correct for highly nonlinear output responses. The LSR creates a regression polynomial of the chosen order such that the sum of the squares of the differences (residues) between the output response values predicted by the regression model and the corresponding simulation model is minimized. MLSM creates a weighted least squares model in which the weights associated with sampling points do not remain constant. The optimal results for the B-pillar SEA and PCF were found using the RBF method, and the R^2 value was found to be 0.97. Accordingly, the RBF method was used to set SEA and PCF design functions for single and multi-objective optimization studies.

Adaptive Response Surface Method (ARSM) [16] and Sequential Quadratic Programming (SQP) [17] optimization methods were used to solve the single-objective optimization problem defined in Eq. (2). ARSM creates response surfaces internally and adaptively updates

them as new assessments become available. SQP is a gradient-based iterative optimization method. Optimization results are given in Table 4.

Table 4. Single-objective optimization results for the B-pillar with tailored properties.

Optimization method	t_u (mm)	t_l (mm)	SEA (kJ/kg)	PCF (kN)
ARSM	0.7	0.75	1.95	69.99
SQP	0.7	0.75	1.95	70

As seen in Table 4, the same optimal results were found for ARSM and SQP methods. SEA value increased by 47.7% from 1.32 to 1.95 kJ/kg compared with the fifth reference design.

Multi-objective Genetic Algorithm (MOGA) and Global Response Surface Method (GRSM) methods were utilized to solve the multi-objective optimization problem defined in Eq. (3), and the Pareto front curves are given in Figures 5 and 6. MOGA is an extension of the Genetic Algorithm that resolves multi-objective optimization problems. GRSM is a response surface-based approach. During each iteration, response surface-based optimization constitutes several designs. Additional designs are formed globally to provide a good balance between local search capability and global search capability. The response surface is adaptively updated with newly constituted designs to fit the model better.

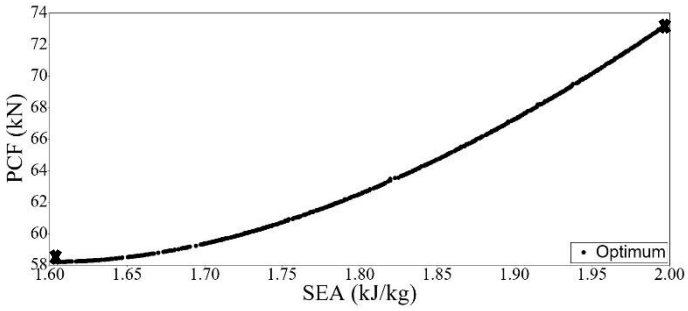

Fig. 5. MOGA Pareto front curve

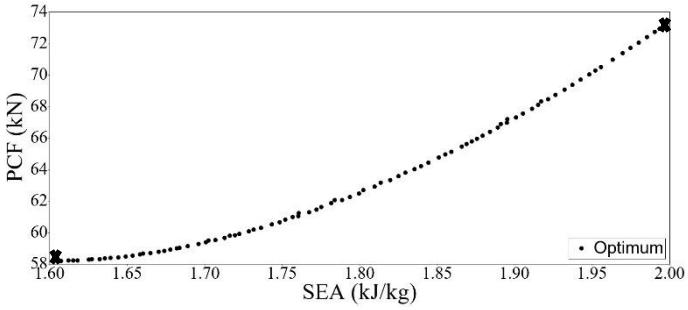

Fig. 6. GRSM Pareto front curve

For both methods, the optimal B-pillar with max SEA increased the SEA by 51.5% from 1.32 to 2.00 kJ/kg compared to the fifth reference design. However, PCF increased 14.9% from 63.7 to 73.2 kN. The increase in SEA undesirably increases the PCF. Similarly, the decrease in PCF decreases the SEA. The results acquired from the solution of Eq. (3) for a single objective (max SEA or min PCF) are given in Table 5. Ideal designs are shown with a cross at the Pareto curves' endpoints in Figures 5 and 6. As seen in Table 5, for min PCF, PCF decreased by 8.6% from 63.7 to 58.2, and SEA increased 21.2% from 1.32 to 1.60 kJ/kg.

Table 5. Ideal designs of two single objective functions for the b-pillar with tailored properties. The ideal optimal results of single objectives are shown in bold and italics

Optimization method	Single-objective	t_u (mm)	t_l (mm)	SEA (kJ/kg)	PCF (kN)
MOGA	Max SEA	0.7	0.7	***2.00***	73.2
	Min PCF	0.7	1.13	1.60	***58.2***
GRSM	Max SEA	0.7	0.7	***2.00***	73.2
	Min PCF	0.7	1.13	1.60	***58.2***

4. Conclusions

Within the study's scope, the impact performance of a boron steel B-pillar with three different hardness values and six different B-pillar designs with tailored properties was compared in crashworthiness. Analysis results were compared regarding specific energy absorption (SEA) and peak crushing force (PCF) values of the B-pillar. For this purpose, single and multi-objective optimization studies were conducted using crash analysis results. The following results were obtained:

The highest SEA value was obtained with 1.33 kJ/kg with the sixth design, whereas 63.7 kN with the fifth design was the lowest PCF value. The SEA value in the fifth design was 1.32 kJ/kg, almost reaching the sixth design. For this reason, the fifth design, "Upper part O25 and lower part T25 heat-treated B-pillar" was used in optimization studies.

The single-objective optimization problem was solved with ARSM and SQP methods. SEA value increased by 47.7% from 1.32 to 1.95 kJ/kg compared with the fifth reference design for both techniques.

MOGA and GRSM methods were utilized to solve the multi-objective optimization problem, and similar Pareto front curves were obtained. For both methods, the optimal B-pillar with max SEA increased the SEA by 51.5% from 1.32 to 2.00 kJ/kg compared to the fifth reference design. However, PCF increased 14.9% from 63.7 to 73.2 kN. The increase in SEA undesirably increases the PCF. Similarly, the decrease in PCF decreases the SEA. This is related to the mechanical properties of the materials and part thicknesses. When Table 5 examined for min PCF, different thickness values were found for the upper and lower parts of the B-pillar. This situation can be expected to increase the cost and complicate the production process.

Nomenclature

SEA	:	spesific energy absorption (kJ/kg)
f(x)	:	impact force (kN)
m	:	mass (kg)
PCF	:	peak crushing force (kN)
t_u	:	Thickness of the O25 heat treated part of the

B-pillar

t_1 : Thickness of the T25 heat treated part of the B-pillar

V : velocity (m/s)

x_{max} : max displacement (m)

Conflict of Interest Statement

The author declares that there is no conflict of interest.

References

[1] Wang D, Dong G, Zhang J, Huang S. Car side structure crashworthiness in pole and moving deformable barrier side impacts. Tinshhua Sci Technol. 2006;11(6):725−730. DOI: 10.1016/S1007-0214(06)70256-5

[2] Njuguna J. The application of energy absorbing structures on side impact protection systems. IJCAT. 2011;40(4):280−287.

[3] Zhang B, Yang J, Zhong Z. Optimisation of vehicle side interior panels for occupant safety in side impact. Int J Crashworthiness. 2010;15(6):617-623, DOI: 10.1080/13588265.2010.484193.

[4] Pan F, Zhu P, Zhang Y. Metamodel-based lightweight design of B-pillar with TWB structure via support vector regression. Comput. Struct. 2010;88(1-2):36-44. DOI: 10.1016/j.compstruc.2009.07.008.

[5] Yang Z, Peng Q, Yang J. Lightweight design of B-pillar with TRB concept considering crashworthiness, L. O' Conner (Ed.): 2012 Third International Conference on Digital Manufacturing and Automation, Conference Publishing Services, Danvers, USA (2012), pp. 510-513, DOI: 10.1109/ICDMA.2012.121.

[6] Cao L, Yao C, Wu H. Reliability optimal design of B-pillar in side impact, Proc. of the SAE 2016 World Congress and Exhibition, SAE International, United States (2016), DOI: 10.4271/2016-01-1523.

[7] Öztürk İ, Kaya N, Öztürk F. Design of vehicle parts under impact loading using a multi-objective design approach. MP. 2018;60(5):501–509. DOI: 10.3139/120.111174.

[8] Li Q, Wu L, Chen T, Li E, Hu L. Multi-objective optimization design of B-pillar and rocker sub-systems of battery electric vehicle. Struct Multidisc Optim. 2021;64:3999–4023. DOI: 10.1007/s00158-021-03073-0.

[9] George R, Worswick M, Detwiler D, Kang, J. Impact Testing of a Hot-Formed B-Pillar with Tailored Properties - Experiments and Simulation. SAE Int. J. Mater. Manf. 2013;6(2):157-162. DOI:10.4271/2013-01-0608.

[10] Worswick MJ, George R, Bardelcik A, Ten Kortenaar L, Detwiler D. Thermal Processing History and Resulting Impact Response of a Hot-Formed Component with Tailored Properties – Numerical Study. AMM. 2014;566:34–40. DOI: 10.4028/www.scientific.net/amm.566.34.

[11] Tang B, Wu F, Wang Q, Li C, Liu J, Ge H. Numerical and experimental study on ductile fracture of quenchable boron steels with different microstructures. Int. J. Lightweight Mater. Manuf. 2020;3(1):55-65. DOI: 10.1016/j.ijlmm.2019.07.001.

[12] Hyperworks 19.0. Radioss Tutorials, Copyright by Altair Engineering Inc., 2019.

[13] Qi C, Sun Y, Yang S. A comparative study on empty and foam-filled hybrid material double-hat beams under lateral impact. Thin-Walled Struct. 2018;129:327-341. DOI: 10.1016/j.tws.2018.04.018

[14] Xiao Z, Mo F, Zeng D, Yang C. Experimental and numerical study of hat shaped CFRP structures under quasi-static axial crushing. Compos. Struct. 2020;249.

[15] J. S. Rao, Kumar B. Three-dimensional shape optimization through design of experiments and meta models in crash analysis of automobiles: Proc. of the Symposium on International Automotive Technology 2013, SAE International, India (2013), pp. 1-13, DOI: 10.4271/2013-26-0032.

[16] Wang G G, Dong Z, Aitchison P. Adaptive response surface method-a global optimization scheme for approximation-based design problems. Eng. Optim. 2021;33(6):707-733. DOI: 10.1080/03052150108940940.

[17] Shi L, Yang R-J, Zhu P. An adaptive response surface method for crashworthiness optimization. Eng. Optim. 2013;45(11):1365-1377. DOI: 10.1080/0305215X.2012.734815.